J Appl Electrochem (2009) 39:1207–1216
DOI 10.1007/s10800-009-9786-5

ORIGINAL PAPER

Effects of temperature and current density on zinc electrodeposition from acidic sulfate electrolyte with [BMIM]HSO_4 as additive

Qi Bo Zhang · Yi Xin Hua · Tie Guang Dong · Dan Gui Zhou

Received: 23 October 2008 / Accepted: 24 December 2008 / Published online: 24 January 2009

Abstract The effects of temperature and current density on cathodic current efficiency, specific energy consumption, and zinc deposit morphology during zinc electrodeposition from sulfate electrolyte in the presence of 1-butyl-3-methylimidazolium hydrogen sulfate ([BMIM]HSO_4) as additive were investigated. The highest current efficiency (93.7%) and lowest specific energy consumption (2,486 kWh t^{-1}) were achieved at 400 A m^{-2} and 313 K with addition of 5 mg dm^{-3} [BMIM]HSO_4. In addition, the temperature dependence of some kinetic parameters for the zinc electrodeposition reaction was experimentally determined. Potentiodynamic polarization sweeps were carried out to obtain the expression for each parameter as a function of temperature. In the condition studied, the exchange current density depended on temperature as $\ln(i_0) = -a/T + b$ and the charge transfer coefficient was constant. Moreover, the adsorption of the additive on cathodic surface obeyed the Langmuir adsorption isotherm. The associated thermodynamic parameters indicated the adsorption to be chemical.

Keywords Temperature · Current density · Additives · Zinc deposition · Ionic liquids

1 Introduction

Over half of the world's zinc is produced from acidic sulfate solutions by electrodeposition [1, 2]. However, electrolysis of zinc is extremely sensitive to the presence of certain metallic impurities [3–6] in the electrolyte, which augment simultaneous evolution of hydrogen during zinc ion electroreduction from aqueous solutions. Hydrogen evolution, which competes for the unit of available current at the cathode with zinc deposition during zinc electrodeposition, decreases cathodic current efficiency and increases specific energy consumption apart from occluding hydrogen into the zinc deposit, thereby increasing internal stress and producing pitted deposits. To achieve high current efficiency and produce a level, smooth, and dense cathodic deposit, the effects of some industrial additives such as glue [7–9], gum arabic [10], and many other additives [11–20] on zinc electrodeposition from acidic sulfate electrolyte have been investigated. Besides, the quality and type of the deposits are found to depend on many other factors [21] such as current density, temperature, pH, zinc concentration, time of electrolysis, agitation, and type of substrate used.

It is known that increasing the current density is expected to result in a higher overpotential, which should increase the nucleation rate [22], thus enhancing the productivity of the electrowinning process [23]. However the current density applied to the electrolysis process is restricted by the limiting current [24], beyond which serious deterioration in the quality of the cathode deposit occurs. In particular, during zinc electrowinning operations, zinc is depleted in the electrolyte solution, while acid increases, which degrades the quality of the cathode deposit and leads to greater acid mist formation. Some types of organic additives have been investigated to prevent acid mist formation [25–27]. Some of these additives are used as leveling agents. Appropriate amounts of these additives are found to be necessary for the formation of fine-grained, smooth, compact deposits. However, most of the literature concentrates on the effects of impurities and additives; scant information is available on the effects of temperature and current density on zinc electrodeposition from sulfate

---

Q. B. Zhang · Y. X. Hua (✉) · T. G. Dong · D. G. Zhou
Faculty of Materials and Metallurgical Engineering, Kunming University of Science and Technology, Kunming 650093, China
e-mail: huayixin@gmail.com

electrolytes, especially with additive in the electrolyte. Scott et al. [28] observed that current efficiency increased with increasing temperature, while energy consumption declined rapidly. Thomas et al. [29] claimed that tetrabutylammonium chloride (TBACL) enabled current densities of up to 2,000 A m^{-2} to be achieved with a current efficiency of around 85% from a zinc chloride electrolyte in a small laboratory cell. Das et al. [15] showed that considerable energy saving in the electrowinning processes could be achieved with increasing operating current density, whilst maintaining high current efficiency and cathode quality.

In our previous report [30], 1-butyl-3-methylimidazolium hydrogen sulfate ([BMIM]HSO_4) was found to be efficient as a leveling agent during zinc electrodeposition from sulfate electrolyte. As an ionic liquid, it may be a potential additive for zinc electrodeposition due to its thermal stability and avirulence [31]. Therefore, it was thought worthwhile to study the effects of temperature and current density on zinc electrodeposition from sulfate electrolyte in presence of [BMIM]HSO_4 as additive. The aim of the present study was to evaluate the effect of temperature and current density on cathodic current efficiency, specific energy consumption, and kinetics of the cathodic process as well as upon the quality of zinc deposits in absence and presence of [BMIM]HSO_4. In addition, the adsorption behavior of the additive during the electrodeposition process is also discussed.

2 Experimental details

2.1 Chemicals

The zinc electrolyte was prepared from AnalaR zinc sulfate ($ZnSO_4 \cdot 7H_2O$) and analytical-grade H_2SO_4. 1-Butyl-3-methylimidazolium hydrogen sulfate ([BMIM]HSO_4) was synthesized in the laboratory as mentioned elsewhere [32, 33]. The electrolytic solution contained 55 g dm^{-3} zinc and 150 g dm^{-3} sulfuric acid, and the specific experimental procedures were similar to as described previously in the literature [17].

2.2 Apparatus

Small-scale galvanostatic electrolysis experiment was performed in a 250 cm^3 plexiglass cell by chronopotentiometric measurements. A pure (>99.95%) aluminum sheet and two parallel lead–silver–calcium–strontium alloy (Ag 0.2%, Ca and Sr 0.1–0.13%) plates of 5 cm^2 were used as the cathode and anode, respectively. The interelectrode distance was 2.5 cm. Zinc was deposited on both sides of the cathode onto a total area of 4.5 cm^2. All the electrowinning experiments were carried out for 2 h at current density ranging from 300 to 600 A m^{-2} with the temperature varying from 303 to 318 K. After electrolysis, the cathode was removed from the cell and washed thoroughly with distilled water and dried. The current efficiency was calculated by weight according to Faraday's law.

A CHI760C electrochemical workstation (Shanghai CH Instruments Company, China) was used for potentiodynamic polarization measurements. A conventional three-electrode cell was used for these experiments. All the potentiodynamic polarization experiments were performed under atmospheric condition and scanned at a constant scan rate of 5 mV s^{-1} from the initial potential of about −1.05 V to the final potential of −1.25 V, and the working temperature was varied from 303 to 318 K. A graphite rod was used as counter, a saturated calomel electrode (SCE) as the reference electrode, and a pure (>99.95%) aluminum sheet (0.3 mm thick) as working electrode. Every sheet was sealed with epoxy resin, with the remaining portion as the efficient working area (0.28 cm^2). Before each electrochemical measurement, ultrapure argon was pumped into the electrolyte for 30 min to remove dissolved oxygen. The aluminum sheet electrode was polished successively with fine-grade emery papers, degreased with anhydrous alcohol in an ultrasonic bath for 10 min, washed with twice-distilled water, and finally dried.

The surface morphology of the deposits was examined by scanning electron microscopy (SEM) using Tescan VEGA II XMH microscope.

3 Results and discussion

3.1 Cathode current efficiency and specific energy consumption

The effects of temperature and current density on current efficiency and specific energy consumption of zinc electrodeposition from acidic sulfate bath in absence and presence of [BMIM]HSO_4 as additive were studied. The results are listed in Table 1.

3.1.1 Effect of temperature

As shown in Table 1, current efficiency increases with increasing temperature, whereas specific energy consumption decreases with increasing temperature. In the presence of 5 mg dm^{-3} [BMIM]HSO_4 in the electrolyte, current efficiency further increases and specific energy consumption decreases. The maximum current efficiency (93.7%) and minimum specific energy consumption (2,486 kWh t^{-1}) were found to occur at 313 K. For constant current density of 400 A m^{-2}, current efficiency increased from 89.8% at

Table 1 Effect of temperature and current density on current efficiency and specific energy consumption during zinc electrodeposition in absence and presence of 5 mg dm^{-3} [BMIM]HSO_4

Current density/A m^{-2}	Temperature/K	Current efficiency/%	Cell voltage/V	Specific energy consumption/kWh t^{-1}
300	303	90.2 (90.9)	2.95 (2.93)	2683 (2644)
	308	90.3 (91.2)	2.92 (2.89)	2653 (2599)
	313	90.6 (92.0)	2.90 (2.86)	2627 (2550)
	318	91.3 (92.8)	2.84 (2.82)	2552 (2493)
400	303	89.8 (92.2)	3.11 (3.08)	2841 (2740)
	308	90.5 (92.5)	2.96 (2.92)	2683 (2589)
	313	90.8 (93.7)	2.89 (2.85)	2611 (2486)
	318	91.7 (93.2)	2.88 (2.84)	2576 (2492)
500	303	90.4 (90.2)	3.15 (3.18)	2858 (2892)
	308	90.9 (90.5)	3.07 (3.15)	2770 (2855)
	313	91.5 (91.7)	3.00 (3.05)	2690 (2728)
	318	92.3 (93.0)	2.95 (2.96)	2622 (2611)
600	303	89.7 (87.7)	3.21 (3.26)	2936 (3049)
	308	90.7 (90.3)	3.12 (3.18)	2822 (2889)
	313	91.8 (91.5)	3.02 (3.13)	2699 (2806)
	318	92.6 (92.4)	2.98 (3.06)	2640 (2728)

Values in parentheses are obtained when 5 mg dm^{-3} [BMIM]HSO_4 is also presence in the electrolyte

303 K to 91.7% at 318 K. With the addition of [BMIM]HSO_4, current efficiency increased by 2.4% in comparison with additive-free solution at 303 K and further increases to 93.2% at 318 K. This increase in current efficiency can be attributed to the fact that high temperatures enhance the rate constants of cathodic reactions [28] and to the suppression of hydrogen evolution and corrosion inhibition of the dissolution of deposited zinc during zinc electrodeposition by blocking of the active sites through cathodic adsorption of additive [20]. On the other hand, the specific energy consumption declined rapidly with increasing temperature (Fig. 1) from 2,841 kWh t^{-1} at 303 K to 2,576 kWh t^{-1} at 318 K. Meanwhile, with addition of 5 mg dm^{-3} [BMIM]HSO_4, a reduction in specific energy consumption of ~100 kWh t^{-1} is obtained at 303 K compared with the additive-free solution. With increasing the temperature to 318 K, an extra specific energy consumption of ~248 kWh t^{-1} is saved in the electrodeposition process. The reason for this decrease in the energy consumption is due both to the increasing current efficiency and the decreasing cell voltage as the temperature rises (Table 1). Cell voltage, which is the voltage drop between adjacent anodic–cathodic electrodes, was found to decrease from 3.11 V at 303 K to 2.88 V at 318 K and from 3.08 V at 303 K to 2.84 V at 318 K for the electrolyte in absence and presence of 5 mg dm^{-3} [BMIM]HSO_4, respectively (Fig. 2). This successive reduction of cell voltage is based on the fact that a lower driving force for cathodic electrodeposition is required at higher temperature, which leads to a decrease in the cathodic potential (Fig. 5a). The cathode potential decreased from ~1.145 V to ~1.080 V between 303 K and 318 K.

3.1.2 *Effect of current density*

Current efficiency was found to be independent of current density over the range from 300 to 600 A m^{-2} at lower temperature (Table 1). Similar results over the range 100–650 A m^{-2} at lower acidity were observed by other workers [28] and were general attributable to the negligible mass transfer resistance (or concentration overpotential) over the range of current densities. At higher temperature, both increase in current efficiency and specific energy consumption are observed (Fig. 3). It is noteworthy that in presence of [BMIM]HSO_4 the current efficiency increased with specific energy consumption decreasing rapidly at

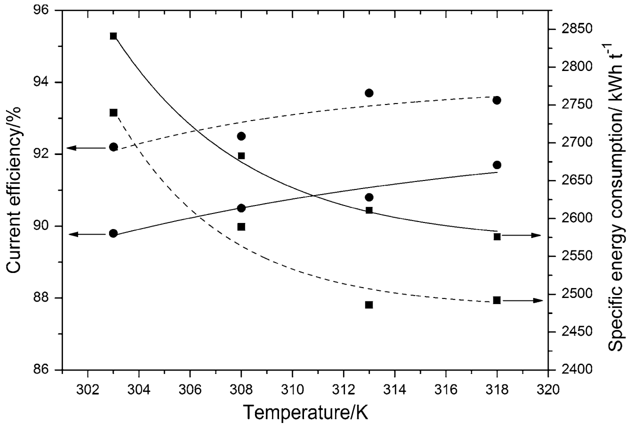

Fig. 1 Effect of temperature on electrodeposition performance; zinc concentration = 55 g L^{-1}; acidity = 150 g L^{-1}; current density = 400 A m^{-2}. (–) Blank, (···) in the presence of 5 mg dm^{-3} [BMIM]HSO_4

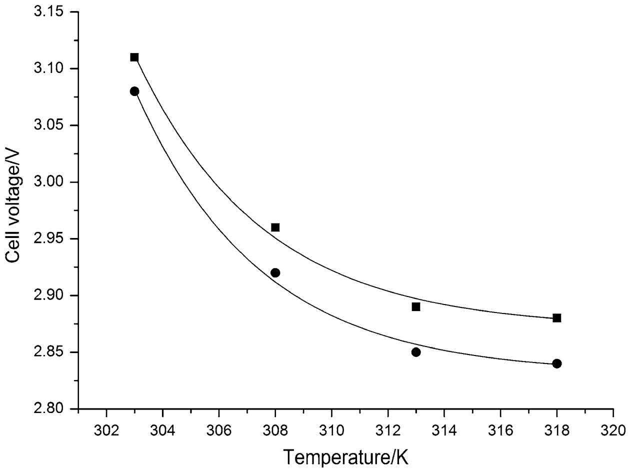

Fig. 2 Effect of temperature on the cell voltage; zinc concentration = 55 g L^{-1}; acidity = 150 g L^{-1}; current density = 400 A m^{-2}. In absence (■) and presence (●) of 5 mg dm^{-3} [BMIM]HSO_4

current density below 500 A m^{-2} compared with the additive-free solution. However, when the current density increases to 500 A m^{-2}, more specific energy consumption is required for the electrodeposition process (Fig. 3); for example, ~88 kWh t^{-1} more specific energy consumption is needed when the current density increases to 600 A m^{-2} at 318 K with the addition of [BMIM]HSO_4 in comparison with the additive-free solution. The increase in specific energy consumption can be attributed to the larger driving force for the electrodeposition process at higher current density, which increases both anodic and cathodic potential with increasing current density, and thus results in increasing cell voltage. Besides, this increase is also related to the increase in the *IR* voltage drop across the solution [28]. The cell voltage was found to increase linearly from 2.84 V at 300 A m^{-2} to 2.98 V at 600 A m^{-2} for the additive-free solution and increase sharply from 2.82 V at 300 A m^{-2} to 3.06 V at 600 A m^{-2} for the solution in presence of 5 mg dm^{-3} [BMIM]HSO_4 (Fig. 4). This increasing trend is found to be more pronounced with the addition of [BMIM]HSO_4 when the current density increases to 500 A m^{-2}, consistent with the energy consumption change discussed above. This could be related to the surface coverage of the cathode by a strongly adsorbed additive layer with the addition of additive, which increases the interfacial viscosity and decreases the mass transfer, and thus a higher driving force for zinc ion reduction is required, in particular at higher current density.

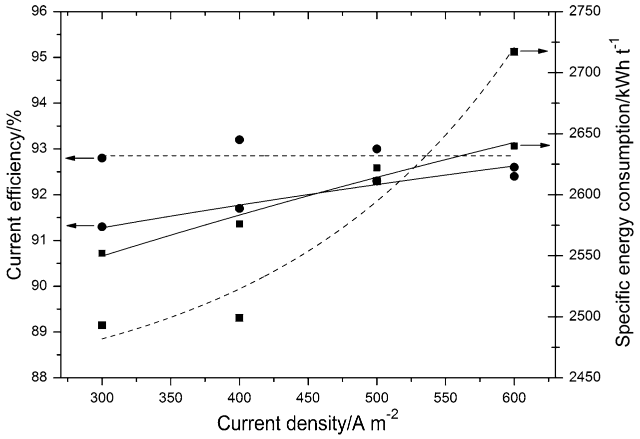

Fig. 3 Effect of current density on the electrodeposition performance; zinc concentration = 55 g L^{-1}; acidity = 150 g L^{-1}; temperature = 318 K. (–) Blank, (···) in the presence of 5 mg dm^{-3} [BMIM]HSO_4

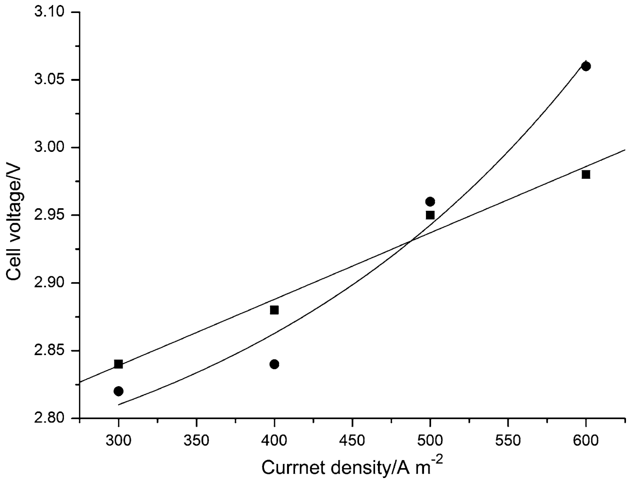

Fig. 4 Effect of current density on the cell voltage; zinc concentration = 55 g L^{-1}; acidity = 150 g L^{-1}; temperature = 318 K. In absence (■) and presence (●) of 5 mg dm^{-3} [BMIM]HSO_4

3.2 Polarization studies

The cathodic potentiodynamic polarization curves for zinc electrodeposition on aluminum electrode from acidic zinc sulfate solutions in absence and presence of different concentrations of [BMIM]HSO_4 at temperature varying range from 303 to 318 K are shown in Fig. 5. An inhibition effect can be noticed because the reduction potential of Zn^{2+} shifts to more negative values in presence of [BMIM]HSO_4. In addition, the effect is more obvious at higher [BMIM]HSO_4 concentration. This can be attributed to the strong adsorption of additive on the cathodic electrode surface and that the adsorption process enhances with increasing additive concentration. On the other hand, increasing temperature promoted a progressive shift of the deposit potential to more positive values. This indicated that the zinc electroreduction is stimulated with increasing temperature, which is consistent with the discussion in the previous section.

The kinetic parameters Tafel slope b (mV $decade^{-1}$), cathodic charge transfer coefficient α_c, and exchange current densities i_0 (mA cm^{-2}) for zinc electrodeposition

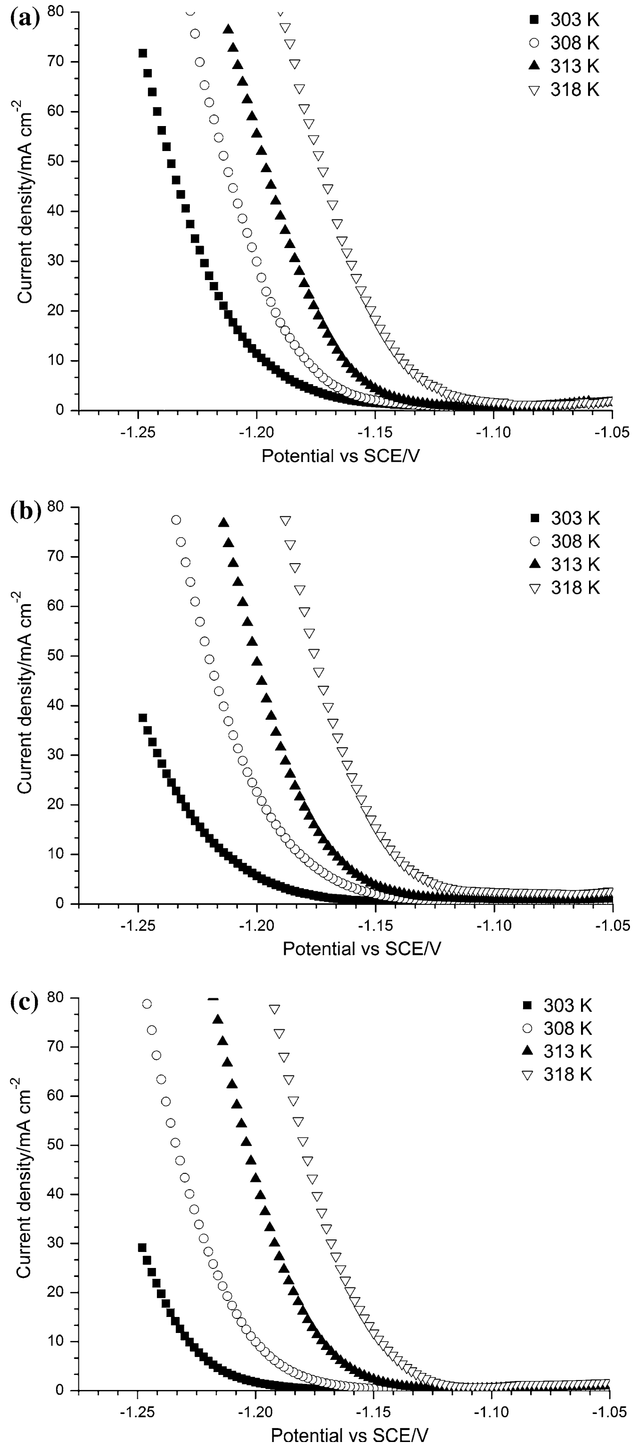

Fig. 5 Effect of temperature on the cathodic polarization during zinc deposition on aluminum in absence and presence of different concentrations of [BMIM]HSO$_4$: **a** blank, **b** 5 mg dm^{-3}, and **c** 10 mg dm^{-3}

on aluminum electrode were calculated from the cathodic potentiodynamic polarization curves using the same method as described previously [17]. The corresponding results are given in Table 2.

3.2.1 Effect of temperature on charge transfer coefficient

As can be seen from Table 2, the cathodic Tafel slope varies from 122 to 139 mV decade^{-1}, whilst the charge transfer coefficient varies between 0.45 and 0.49 in absence and presence of different concentrations of [BMIM]HSO$_4$ in the temperature range from 303 to 318 K. Small changes in Tafel slope and charge transfer coefficient indicate that this additive does not control the charge transfer reaction [19, 30]. The charge transfer coefficient α values from Table 2 are plotted against temperature in Fig. 6. α is practically constant over the studied temperature range and, taking into account the effect of additive, could be calculated as

$$\alpha = 0.485 - 0.003c \pm 0.005, \qquad (1)$$

where c is the concentration of additive (mg dm^{-3}). The correlation coefficient is 0.96. The experimental and the estimated charge transfer coefficients are illustrated in Fig. 7. The slight sigmoid shape around the ideal 45° line indicates that this estimation is in reasonable agreement. As this coefficient depends on the reaction mechanism, it becomes apparent that the mechanism for zinc electrodeposition does not change with temperature in the studied temperature range.

3.2.2 Effect of temperature on the exchange current density

The exchange current density, i_0 (mA cm^{-2}) is found to progressively increase with increasing temperature and this effect is more pronounced at higher temperature. The obtained results also show that presence of [BMIM]HSO$_4$ has an inhibition effect on the kinetics of the Zn^{2+} reduction process, indicated by the decrease of the exchange current density at a given temperature. The inhibition enhancement was due to increasing additive concentration, which could be related to the strong adsorption of additive on the cathodic electrode surface. This adsorption results in the blocking of the active nucleation sites of the cathode surface.

In addition, various relationships between the exchange current density for the cathodic reaction and the absolute temperature (K) were tried. A linear fit is found between the logarithm of the exchange current density (values in Table 2) and the reciprocal value of the absolute temperature. The plot is shown in Fig. 8.

The numerical relationship was obtained with Origin software as

$$\ln(i_0) = -a/T + b, \qquad (2)$$

where a and b are the slope and the intercept of the straight lines, respectively. The correlation coefficient is 0.999.

Table 2 Effects of temperature on the kinetic parameters during zinc electrodeposition in absence and presence of different concentrations of [BMIM]HSO_4

Temperature/K	Concentration/ mg dm^{-3}	Tafel slope/mV $decade^{-1}$	Transfer coefficient, α_c	Exchange current density, i_0/mA cm^{-2} ($\times 10^{-2}$)	Surface coverage, θ
[BMIM]HSO_4					
303	Blank	122	0.492	7.83	–
	1	124	0.484	5.46	0.303
	2	126	0.477	5.21	0.335
	5	130	0.462	4.89	0.377
	10	133	0.452	4.67	0.403
308	Blank	125	0.488	16.4	–
	1	127	0.481	11.2	0.318
	2	128	0.477	10.6	0.352
	5	133	0.459	9.74	0.406
	10	135	0.452	9.18	0.441
313	Blank	127	0.488	39.3	–
	1	129	0.481	25.1	0.362
	2	130	0.477	23.1	0.413
	5	134	0.463	20.0	0.490
	10	137	0.453	18.3	0.535
318	Blank	129	0.489	82.0	–
	1	131	0.484	51.5	0.372
	2	134	0.470	47.6	0.419
	5	136	0.463	41.0	0.500
	10	139	0.453	36.7	0.553

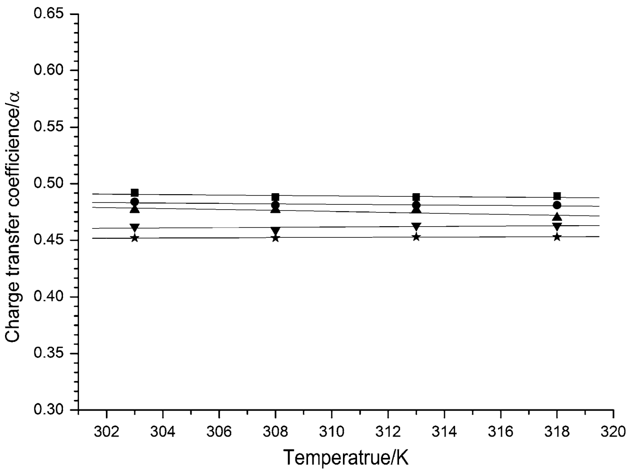

Fig. 6 Transfer coefficient as a function of temperature for the Zn^{2+}/Zn^0 reaction in the absence and presence of different concentrations of [BMIM]HSO_4: (■) blank, (●) 1 mg dm^{-3}, (▲) 2 mg dm^{-3}, (▼) 5 mg dm^{-3}, and (★) 10 mg dm^{-3}

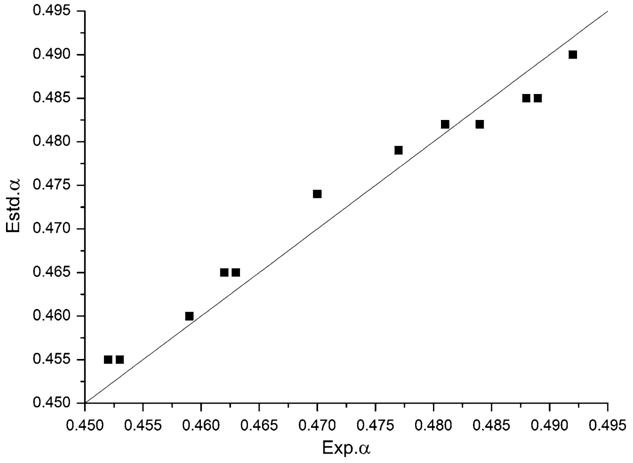

Fig. 7 Experimental (Exp.) and predicted (Estd.) α values obtained by Eq. 1

This relationship is typical of mixed control as described previously [34] and is given by

$$\ln i_{0c} = -\frac{\alpha_c F|\eta_c|}{R}\frac{1}{T} + \ln\left|\frac{i_c i_{Lc}}{(i_c - i_{Lc})}\right|, \tag{3}$$

where i_c, i_{0c}, and i_{Lc} are the cathodic cell current density, cathodic exchange current density, and cathodic limiting current density, respectively, α_c is the cathodic charge transfer coefficient, η_c is the cathodic overpotential, F is Faraday's constant, and R is the gas constant. Equation 3 essentially exhibits the same behavior as Eq. 2 as the second term on the right-hand side of Eq. 3 remains fairly constant with temperature. After comprehensive consideration of the effect of the additive concentration, the numerical relationship can be expressed as

$$\ln(i_0) = -(14,570 - 139.35c)/T - 0.476c + 37.038, \tag{4}$$

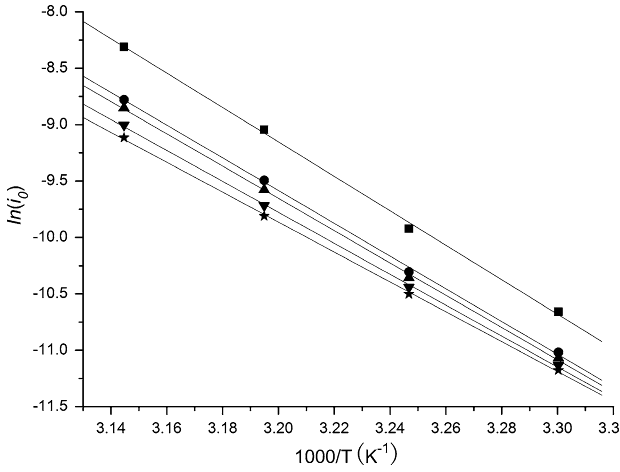

Fig. 8 Logarithm of exchange current density (i_0) as a function of 1,000/T for Zn^{2+}/Zn^0 reaction in absence and presence of different concentrations of [BMIM]HSO_4: (■) blank, (●) 1 mg dm^{-3}, (▲) 2 mg dm^{-3}, (▼) 5 mg dm^{-3}, and (★) 10 mg dm^{-3}

where c is the additive concentration (mg dm^{-3}). The correlation coefficient is 0.96. The experimental and the estimated results are also compared and shown in Fig. 9. The slight deviation around the ideal 45° line also indicated that this estimation is in reasonable agreement.

3.3 Adsorption isotherm

In order to get more information on the mode of adsorption of the additive on the metal surface at different concentrations, the degree of surface coverage, θ, as a function of additive concentration was taken into account. The surface coverage (θ) is calculated by using the following relationship and the corresponding values are listed in Table 2:

$$\theta = \frac{i_0 - i_{0(\text{add})}}{i_0}, \tag{5}$$

where i_0 and $i_{0(\text{add})}$ are the exchange current density without and with addition of additive, respectively, determined by extrapolation of Tafel line to the zero overpotential.

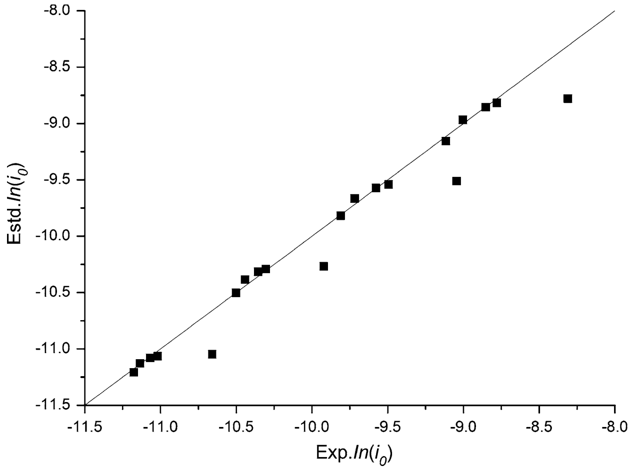

Fig. 9 Experimental (Exp.) and predicted (Estd.) ln(i_0) values obtained from Eq. 4

The straight line obtained on plotting log $\theta/(1-\theta)$ versus log c as shown in Fig. 10 suggests that the adsorption of the additive on the cathodic surface in the zinc acidic sulfate electrolyte solution follows Langmuir's adsorption isotherm. The mode of adsorption of the additive on the electrode surface does not change with temperature in the studied range.

The free energy of adsorption (ΔG_{ads}) was calculated from the equation [35]:

$$\Delta G_{\text{ads}} = -RT\ln(55.5K_{\text{ads}}), \tag{6}$$

where 55.5 mol dm^{-3} is the molar concentration of water in the solution, R is the gas constant, T is the absolute temperature, and K_{ads} is the equilibrium constant, given by

$$K_{\text{ads}} = \frac{\theta}{c(1-\theta)}. \tag{7}$$

The corresponding data obtained in the presence of 2 mg dm^{-3} additive at different temperatures are given in Table 3. The absolute values of free energy of adsorption (ΔG_{ads}) calculated in presence of additive are found to be relatively high and more than 40 kJ mol^{-1} and increase with increasing temperature. Since the value of ΔG_{ads} of -40 kJ mol^{-1} is usually accepted as a threshold value between chemisorption and physisorption [36]. The results reflect strong chemisorption of the additive on the cathodic surface and their negative sign indicates spontaneous interaction of additive molecule with the aluminum electrode surface. On the other hand, the equilibrium constant increases with increasing temperature, also suggesting that this additive is chemisorptive on the electrode surface.

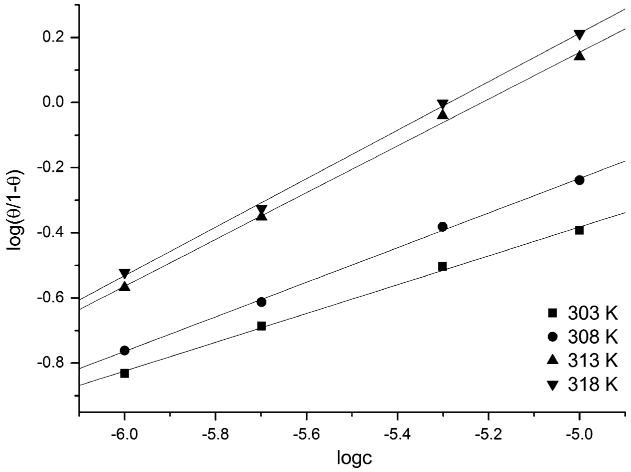

Fig. 10 The Langmuir isotherm for the adsorption of the additive on the aluminum electrode surface in the zinc acidic sulfate electrolyte solution at different temperatures

Table 3 Equilibrium constant and free energy of adsorption for aluminum in the zinc acidic sulfate electrolyte solution in the presence of 2 mg dm^{-3} [BMIM]HSO_4 at different temperatures

Temperature/K	$(10^{-3})\ K_{ads}$	$-\Delta G_{ads}$/kJ mol^{-1}
303	251.9	41.45
308	271.0	42.32
313	351.8	43.69
318	361.1	44.45

3.4 Deposit morphology

The effects of temperature and current density on the zinc deposits in absence and in presence of [BMIM]HSO_4 as additive were examined using scanning electron microscopy (SEM). Typical SEM photomicrographs are shown in Figs. 11 and 12.

It is clear that the deposit obtained from addition-free solution consisted of hexagonal platelets of moderate size and the platelet size progressively decreased with increasing temperature. Addition of 5 mg dm^{-3} [BMIM]HSO_4 to the solution produced a compact and smooth morphology along with a significant reduction in platelet size. Such changes were also reflected in the current efficiency and specific energy consumption. In addition, although a similar law has been observed with increasing current density, the effect of grain refinement is not obvious, in particular when the current density exceeds 500 A m^{-2}. This is consistent with high reaction resistance and the increase in specific energy

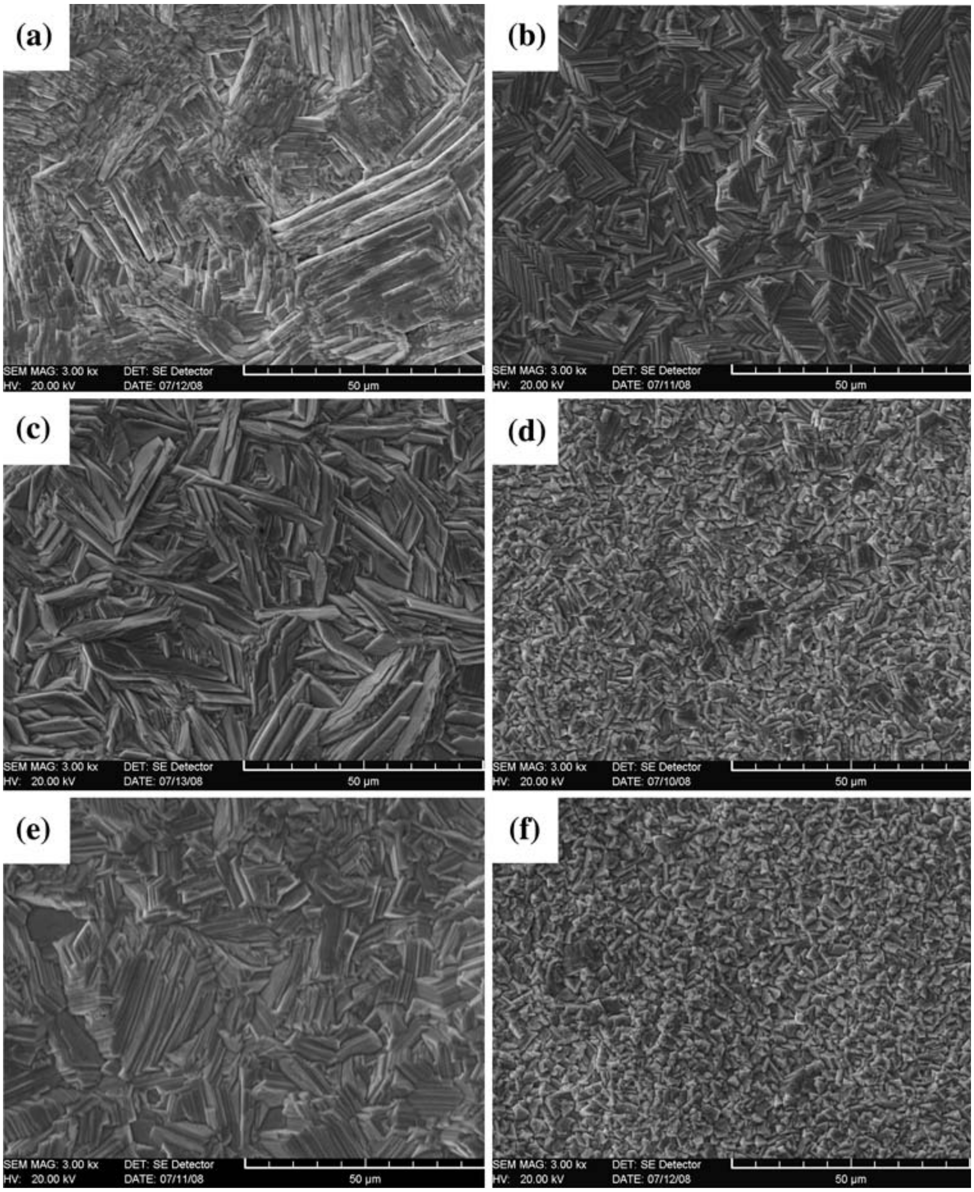

Fig. 11 SEM micrographs of zinc deposits at 400 A m^{-2} in absence and presence of [BMIM]HSO_4 with different temperatures: **a** blank, 303 K; **b** [BMIM]HSO_4—5 mg dm^{-3}, 303 K; **c** blank, 313 K; **d** [BMIM]HSO_4—5 mg dm^{-3}, 313 K; **e** blank, 318 K; **f** [BMIM]HSO_4—5 mg dm^{-3}, 318 K

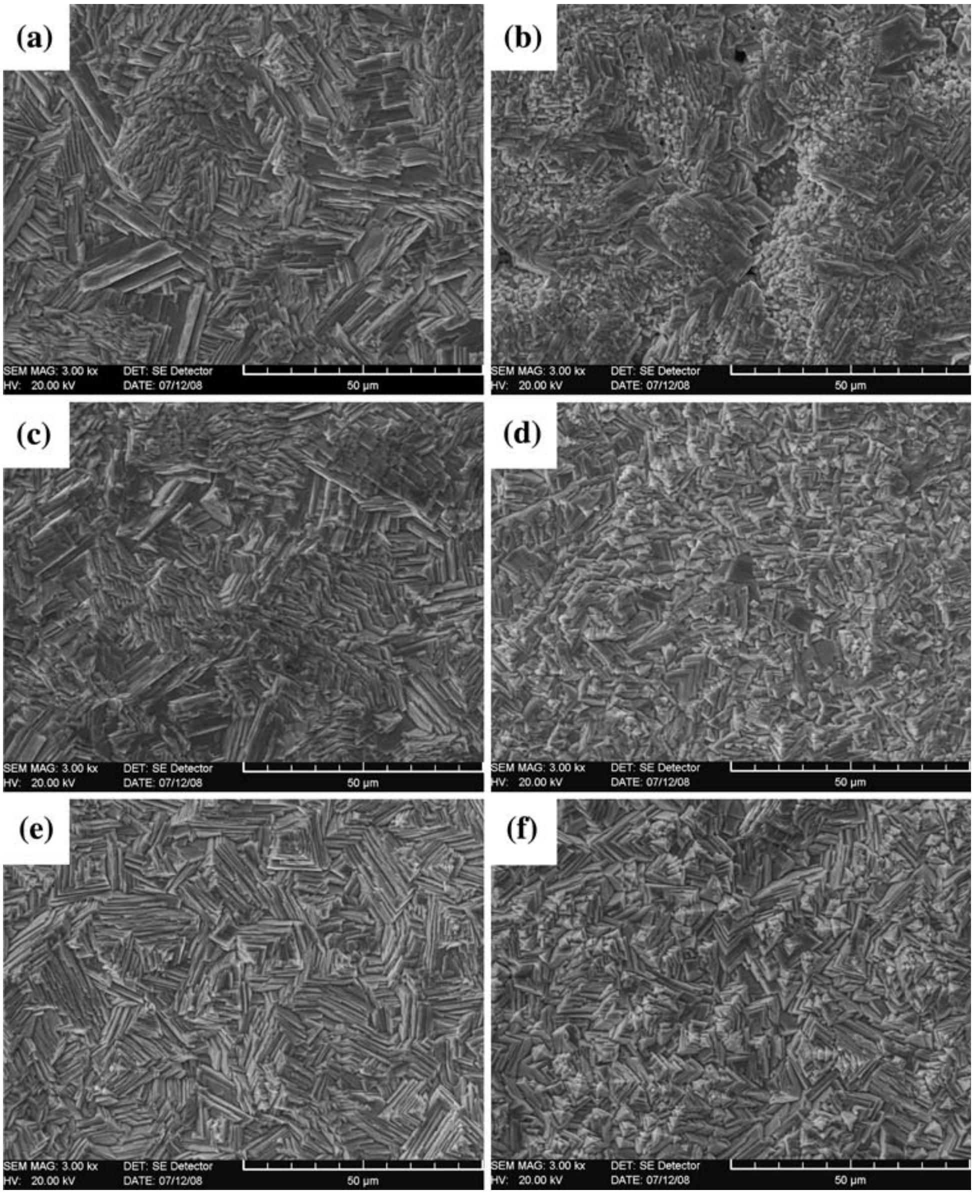

Fig. 12 SEM micrographs of zinc deposits at 313 K in absence and presence of [BMIM]HSO$_4$ with different current densities: **a** blank, 300 A m^{-2}; **b** [BMIM]HSO$_4$—5 mg dm^{-3}, 300 A m^{-2}; **c** blank, 500 A m^{-2}; **d** [BMIM]HSO$_4$—5 mg dm^{-3}, 500 A m^{-2}; **e** blank, 600 A m^{-2}; **f** [BMIM]HSO$_4$—5 mg dm^{-3}, 600 A m^{-2}

consumption observed in the current density beyond 500 A m^{-2} as discussed in the previous section. In all cases with addition of [BMIM]HSO$_4$, the grain refinement showed clearly that inhibition of the electrocrystallization process took place. The action of [BMIM]HSO$_4$ is one of inhibition of the crystal growth process, so that a relative enhancement of the nucleation process is induced [37]. This results in a finer-grained deposit.

4 Conclusions

The objective of this study was to investigate the effect of temperature and current density on zinc electrodeposition from sulfate electrolyte in presence of [BMIM]HSO$_4$ as additive. Analysis of the results led to the following conclusions:

(i) Increasing the temperature results in reduction in the average crystallite size of the zinc deposits. This phenomenon is associated with an increase in the deposition efficiency and a drop in the specific energy consumption. The changes become more obvious with the addition of [BMIM]HSO$_4$ and are suggested as being responsible for the inhibition of the electrocrystallization process and dissolution of deposit zinc.

(ii) Similar effect on the gain refinement of zinc deposit is obtained with increasing current density. At lower current density, the current efficiency further increases along with a marked decline of specific energy consumption with the addition of [BMIM]HSO$_4$, but more specific energy consumption is needed when the current density exceeds 500 A m^{-2}.

(iii) The cathodic polarization of zinc increases with increasing [BMIM]HSO_4 concentration and decreases with increasing temperature. In all cases addition of [BMIM]HSO_4 was found to have an inhibiting effect on the kinetics of the Zn^{2+} reduction process.

(iv) The kinetic parameter values obtained from the experimental potentiodynamic polarization measurements and the estimation expressions for the calculation of these parameters are in good agreement.

(v) The charge transfer coefficient values for the Zn^{2+}/Zn^0 reaction slightly decrease with an increase in the additive concentration, but do not significantly change with temperature; its value is

$$\alpha = 0.485 - 0.003c \pm 0.005.$$

(vi) The exchange current density for the Zn^{2+}/Zn^0 reaction depends on temperature and the additive concentration as

$$\ln(i_0) = -(14{,}570 - 139.35c)/T - 0.476c + 37.038.$$

(vii) The associated thermodynamic parameters indicate that the additive is chemisorption on the cathodic surface and that the adsorption obeys the Langmuir's adsorption isotherm.

Acknowledgements The authors gratefully acknowledge the financial support of the National Natural Science Foundation of China (Project No. 50564006) and the Natural Science Foundation of Yunnan Province (Project No. 2005E0004Z).

References

1. Gurmen S, Emre M (2003) Minerals Eng 16:559
2. Beshore AC, Flori BJ, Schade G, O'Keefe TJ (1987) J Appl Electrochem 17:765
3. Mackinnon DJ, Brannen JM, Kerby RC (1979) J Appl Electrochem 9:55
4. Mackinnon DJ, Brannen JM, Kerby RC (1979) J Appl Electrochem 9:71
5. Ault AR, Frazer EJ (1988) J Appl Electrochem 18:583
6. Muresan L, Maurin G, Oniciu L, Gaga D (1996) Hydrometallurgy 43:345
7. Robinson DJ, O'Keefe TJ (1976) J Appl Electrochem 6:1
8. Mackinnon DJ, Brannen JM, Fenn PL (1987) J Appl Electrochem 17:1129
9. Mackinnon DJ, Morrison RM, Mouland JE, Warren PE (1990) J Appl Electrochem 20:728
10. Sato R (1959) J Electrochem Soc 106:206
11. Piron DL, Mathieu D, Amboise MD (1981) Can J Chem Eng 65:685
12. Hosny AY (1993) Hydrometallurgy 34:361
13. Karavasteva M, Karaivanov SA (1993) J Appl Electrochem 23:763
14. Karavasteva M (1994) Hydrometallurgy 35:391
15. Das SC, Singh P, Hefter GT (1996) J Appl Electrochem 26:1245
16. Das SC, Singh P, Hefter GT (1997) J Appl Electrochem 27:738
17. Tripathy BC, Das SC, Singh P, Hefter GT (1997) J Appl Electrochem 27:673
18. Tripathy BC, Das SC, Singh P, Hefter GT (1999) J Appl Electrochem 29:1229
19. Tripathy BC, Das SC, Hefter GT, Singh P (1998) J Appl Electrochem 28:915
20. Tripathy BC, Das SC, Singh P, Hefter GT, Misra VN (2004) J Electroanal Chem 565:49
21. Winand R (1991) J Appl Electrochem 21:377
22. Ebrahimi F, Ahmed Z (2003) J Appl Electrochem 33:733
23. Ilkhchi MO, Yoozbashizadeh H, Safarzadeh MS (2007) Chem Eng Process 46:757
24. Saba AE, Elsherief AE (2000) Hydrometallurgy 54:91
25. Gonzalez-Domingnuez JA & Lew RW (1995) J Metal 47:34
26. Hosny AY (1993) Hydrometallurgy 32:261
27. Lamping BA, O'Keefe TJ (1976) Met Trans B 7B:551
28. Scott AC, Pitblado RM, Braton GW, Ault AR (1988) J Appl Electrochem 18:120
29. Thomas BK, Fray DJ (1981) J Appl Electrochem 11:677
30. Zhang QB, Hua YX (2008) Effects of 1-Butyl-3-methylimidazolium hydrogen sulfate-[BMIM]HSO_4 on zinc electrodeposition from acidic sulfate electrolyte. J Appl Electrochem. doi:10.1007/s10800-008-9665-5
31. Earle MJ, Seddon KR (2000) Pure Appl Chem 72:1391
32. Huddleston JG, Visser AE, Reichert WM, Willauer HD, Broker GA, Rogers RD (2001) Green Chem 3:156
33. Whitehead JA, Lawrance GA, McCluskey A (2004) Aust J Chem 57:151
34. Cifuentes L, Simpson J (2005) Chem Eng Sci 60:4915
35. Cases JM, Villieras F (1992) Langmuir 8:1251
36. Yurt A, Ulutas S, Dal H (2006) Appl Surf Sci 253:919
37. Varvara S, Muresan L, Nicoar A, Maurin G, Popescu IC (2001) Mater Chem Phys 72:332